



**HAL**  
open science

# Development and pilot-scale validation of a fuzzy-logic control system for optimization of methane production in fixed-bed reactors

Gabriel Capson-Tojo, M. V. Ruano, Eric Latrille, Jean-Philippe Steyer

► **To cite this version:**

Gabriel Capson-Tojo, M. V. Ruano, Eric Latrille, Jean-Philippe Steyer. Development and pilot-scale validation of a fuzzy-logic control system for optimization of methane production in fixed-bed reactors. *Journal of Process Control*, 2018, 68, pp.96-104. 10.1016/j.jprocont.2018.05.007 . hal-04182261

**HAL Id: hal-04182261**

**<https://hal.inrae.fr/hal-04182261>**

Submitted on 17 Aug 2023

**HAL** is a multi-disciplinary open access archive for the deposit and dissemination of scientific research documents, whether they are published or not. The documents may come from teaching and research institutions in France or abroad, or from public or private research centers.

L'archive ouverte pluridisciplinaire **HAL**, est destinée au dépôt et à la diffusion de documents scientifiques de niveau recherche, publiés ou non, émanant des établissements d'enseignement et de recherche français ou étrangers, des laboratoires publics ou privés.

Manuscript Number:

Title: Development and pilot-scale validation of a fuzzy-logic control system for optimization of methane production in fixed-bed reactors

Article Type: Research Paper

Keywords: Anaerobic digestion, bio-methane, fixed-bed reactor, fuzzy-logic control, optimization, winery wastewater

Corresponding Author: Dr. Angel Robles, Ph.D.

Corresponding Author's Institution: Universitat Politècnica de València

First Author: Angel Robles, Ph.D.

Order of Authors: Angel Robles, Ph.D.; Gabriel Capson-Tojo, M.Sc.; María Victoria Ruano, Ph.D.; Eric Latrille, Ph.D.; Jean-Philippe Steyer, Ph.D.

Abstract: The objective of this study was to develop an advanced control system for optimizing the performance of fixed-bed anaerobic reactors. The controller aimed at maximizing the bio-methane production whilst controlling the volatile fatty acids content in the effluent. For this purpose, a fuzzy-logic controller was developed, tuned and validated in an anaerobic fixed-bed reactor at pilot scale (350 litres) treating raw winery wastewater. The results showed that the controller was able to adequately optimize the process performance, maximizing the methane production, with an average methane yield of about 0.29 LCH<sub>4</sub> g<sup>-1</sup> COD. On the other hand, the controller maintained the volatile fatty acids content in the effluent close to the established maximum limit (750 mg COD L<sup>-1</sup>). The outcomes of this study are expected to facilitate plant engineers to establish an optimal control strategy that enables an adequate process performance with the maximum bio-methane productivity.

Dear Editor,

Attached you will find the manuscript entitled “**Development and pilot-scale validation of a fuzzy-logic control system for optimization of methane production in fixed-bed reactors**” submitted for consideration as a research paper in Journal of Process Control. All the authors mutually agree for submitting this manuscript to Journal of Process Control. We confirm that it is the original work and that the work presented has not been submitted earlier to this Journal.

The main objective of this work was to develop an advanced control system for optimizing the performance of fixed-bed anaerobic reactors. The controller aimed at maximizing the bio-methane production whilst controlling the volatile fatty acids content in the effluent. To this aim, a fuzzy-logic controller was developed, tuned and validated in an anaerobic fixed-bed reactor at pilot scale treating raw winery wastewater. The outcomes of this study are expected to facilitate plant engineers to establish an optimal control strategy that enables an adequate process performance with the maximum bio-methane productivity.

The important findings that must be highlighted are:

- Simulation results show that the proposed controller is capable to achieve great process performances even when operating at high VFA concentrations.
- The controller was sufficient to capture the dynamics of the process around the corresponding set point.
- Pilot results showed the potential of this control approach to maintain the process working properly under similar conditions to the ones expected at full-scale plants.

Yours sincerely,

Ángel Robles Martínez, PhD

CALAGUA – Unidad Mixta UV-UPV

Departament d'Enginyeria Química, ETSE-UV.

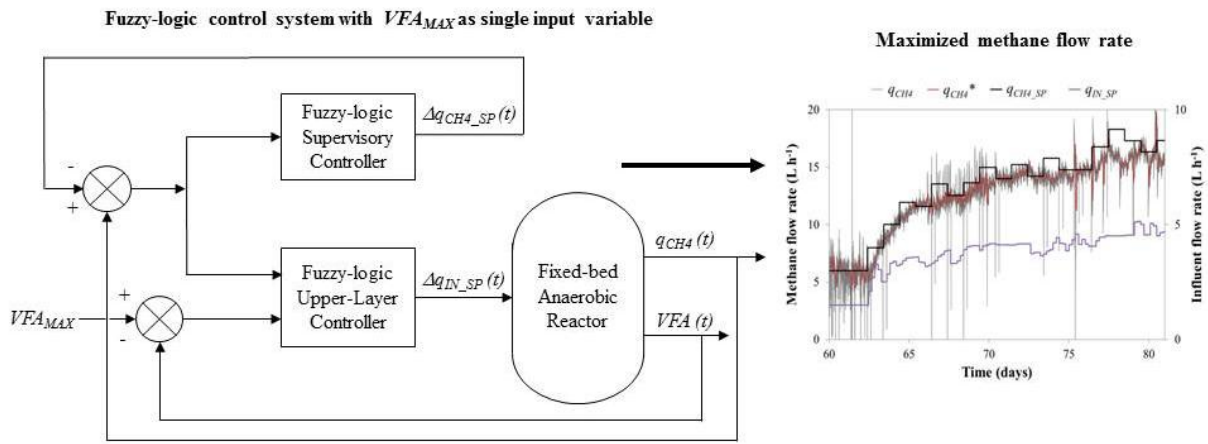
Universitat de València

Avinguda de la Universitat s/n, 46100, Burjassot, València, Spain

Tel.: +34 96 354 30 85

E-mail: angel.robles@uv.es

1 **Graphical abstract**



2

1           **Highlights**

- 2           • A fuzzy-logic control system for optimizing the methane production was proposed
- 3           • The controller was developed, tuned and validated at a 350 L pilot-scale system
- 4           • The controller aimed to maximize methane production whilst controlling VFA
- 5           contents
- 6           • Methane yields up to  $0.29 \text{ L CH}_4 \text{ g}^{-1} \text{ COD}$  were achieved when running the
- 7           controller

1                    **Development and pilot-scale validation of a fuzzy-logic control**  
2                    **system for optimization of methane production in fixed-bed reactors**

3                    A. Robles<sup>a,b,\*,\*\*</sup>, G. Capson-Tojo<sup>b</sup>, M.V. Ruano<sup>c</sup>, E. Latrille<sup>b</sup> and J.-P. Steyer<sup>b</sup>

4  
5                    <sup>a</sup> CALAGUA – Unidad Mixta UV-UPV, Institut Universitari d'Investigació  
6                    d'Enginyeria de l'Aigua i Medi Ambient – IIAMA, Universitat Politècnica de  
7                    València, Camí de Vera s/n, 46022, València, Spain. (E-mail: *ngeroema@upv.es*)

8                    <sup>b</sup> LBE, INRA, 102 avenue des Etangs, 11100, Narbonne, France. (E-mail:  
9                    *gabriel.capson-tojo@supagro.inra.fr; eric.latrille@inra.fr; jean-*  
10                    *philippe.steyer@inra.fr*)

11                    <sup>c</sup> CALAGUA – Unidad Mixta UV-UPV, Departament d'Enginyeria Química, ETSE-  
12                    UV, Universitat de València, Avinguda de la Universitat s/n, 46100, Burjassot,  
13                    València, Spain. (E-mail: *m.victoria.ruano@uv.es*)

14                    \* Corresponding author: Tel.: +34 96 354 30 85; E-mail: *angel.robles@uv.es*

15                    \*\* *Current address: CALAGUA – Unidad Mixta UV-UPV, Departament*  
16                    *d'Enginyeria Química, ETSE-UV, Universitat de València, Avinguda de la*  
17                    *Universitat s/n, 46100, Burjassot, València, Spain. (E-mail: *angel.robles@uv.es*)*

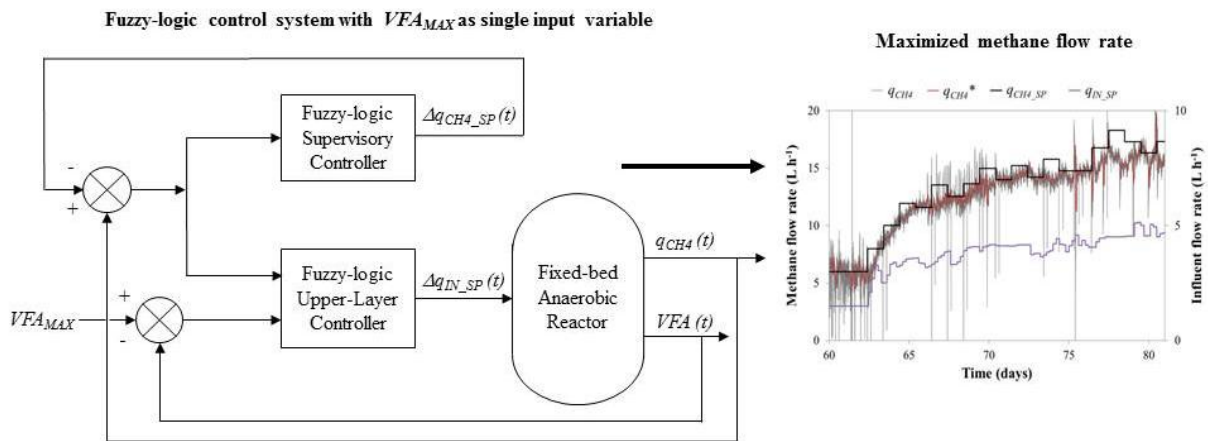
18  
19                    **Abstract**

20                    The objective of this study was to develop an advanced control system for optimizing  
21                    the performance of fixed-bed anaerobic reactors. The controller aimed at maximizing  
22                    the bio-methane production whilst controlling the volatile fatty acids content in the  
23                    effluent. For this purpose, a fuzzy-logic controller was developed, tuned and  
24                    validated in an anaerobic fixed-bed reactor at pilot scale (350 litres) treating raw

25 winery wastewater. The results showed that the controller was able to adequately  
 26 optimize the process performance, maximizing the methane production, with an  
 27 average methane yield of about  $0.29 \text{ L}_{\text{CH}_4} \text{ g}^{-1} \text{ COD}$ . On the other hand, the controller  
 28 maintained the volatile fatty acids content in the effluent close to the established  
 29 maximum limit ( $750 \text{ mg COD L}^{-1}$ ). The outcomes of this study are expected to  
 30 facilitate plant engineers to establish an optimal control strategy that enables an  
 31 adequate process performance with the maximum bio-methane productivity.

32

33 **Graphical abstract**



34

35 **Keywords**

36 Anaerobic digestion, bio-methane, fixed-bed reactor, fuzzy-logic control,  
 37 optimization, winery wastewater

38

39 **Highlights**

- 40 • A fuzzy-logic control system for optimizing the methane production was proposed
- 41 • The controller was developed, tuned and validated at a 350 L pilot-scale system
- 42 • The controller aimed to maximize methane production whilst controlling VFA
- 43 contents

- 44           • Methane yields up to 0.29 L CH<sub>4</sub> g<sup>-1</sup> COD were achieved when running the  
45           controller

46

## 47 **1. Introduction**

48

49           Nowadays, a major issue to overcome in order to achieve a global sustainable  
50           development is our dependency on fossil fuels for electricity production, which represents up  
51           to 80 % of the global energy consumption [1]. Therefore, one of the main challenges of this  
52           century is to develop new competitive sources of renewable energy, capable of replacing  
53           fossil fuels with a minimum impact on both environment and society [2]. In this context,  
54           alternative energy sources must be pursued [3]. Bio-methane production from anaerobic  
55           digestion (AD) of waste represents a promising option that can be considered as carbon  
56           neutral due to its net balance of greenhouse gases emissions.

57

58           Due to the high methane productivities that can be achieved by high-rate anaerobic  
59           reactors, a huge effort is currently being put on the study of systems such as up-flow  
60           anaerobic sludge blanket (UASB), expanded granular sludge blanket (EGSB), anaerobic  
61           membrane bioreactor (AnMBR) or fixed-bed bioreactor [4]. In these reactors, the biomass is  
62           self-immobilized, allowing uncoupling the hydraulic retention time (HRT) and the solid  
63           retention time (SRT).

64

65           However, the complexity and the diversity of the phenomena occurring in high-rate  
66           anaerobic reactors have delayed the understanding, and consequently the proper control, of  
67           this AD process. Due to the large number of factors that affect anaerobic processes, the  
68           selection of proper monitoring indicators and the development of advanced control systems



69 are crucial for a successful optimization of the process performance [5,6].

70

71 Biogas composition and production rate are the most commonly used variables acting as  
72 indicators of the process performance during AD. In addition, the methane yield ( $Y_{CH_4}$ ),  
73 which is usually defined as the amount of methane produced per unit of organic matter  
74 removed, is also used as an indirect parameter for evaluating the performance of anaerobic  
75 processes [7,8]. Nevertheless, these indicators can be insufficient to evaluate the overall  
76 process performance. This is because they usually indicate too late disturbances affecting the  
77 process, when there is no possible action to recover it immediately. To avoid this issue, the  
78 concentration of volatile fatty acids (VFA) has been proved to be an adequate state indicator  
79 for monitoring AD processes [9]. VFAs are main intermediate metabolites in AD and  
80 therefore, monitoring their concentration can be a useful tool for process diagnosis (*e.g.* to  
81 detect AD imbalances). Moreover, as this variable can be easily on-line monitored, for  
82 instance by means of titrimetric sensors, it gives a much faster and more reliable information  
83 than other common indicators applied for AD monitoring, such as pH, alkalinity, gas  
84 composition or gas production [10–14].

85

86 Many different alternatives, such as classical Proportional-Integral-Derivative (PID)  
87 control, fuzzy systems, neuron networks or model-based systems, have been applied for  
88 controlling AD process [15]. Among these strategies, fuzzy-logic control has the main  
89 advantage of being applicable to control non-linear systems, such as AD. A fuzzy-logic  
90 controller [16] is able to optimize different types of processes under dynamic conditions by  
91 applying valuable expert knowledge [17–20]. Moreover, fuzzy-logic controllers do not  
92 require large amounts of data and/or rigorous mathematical models, thus allowing a much  
93 simpler calibration of the controller. In addition, these control systems allow the development

94 of multiple-input-multiple-output control schemes. Hence, it can be stated that fuzzy logic is a  
95 powerful tool for controlling anaerobic fixed-film reactors [21]. Therefore, fuzzy-logic  
96 control has been widely implemented in wastewater treatment over the last decades and has  
97 been successfully featured in several AD applications [22–26]. As listed in Jimenez et al. [15],  
98 different applications of fuzzy-logic control systems for AD control can be found in the  
99 literature. Taking some examples, Puñal et al [27] developed a PI-based fuzzy-logic controller  
100 which used the dilution rate as manipulated variable to control the concentration of VFAs in  
101 the effluent. In addition, Murnleitner et al. [28] applied fuzzy theory to avoid overloading of  
102 AD reactors. Recently, Robles et al. [29] demonstrated the suitability of fuzzy-logic systems  
103 for controlling the methane production in AD reactors using the methane flow rate and the  
104 VFA concentration as input variables. Nevertheless, only one study has been carried out so far  
105 for optimization of AD processes using fuzzy logic. Carlos-Hernandez et al. [30] proposed a  
106 fuzzy supervisory controller to optimize the AD performance by controlling alkali addition  
107 and the dilution rate. To the knowledge of the authors, no other study has been carried out to  
108 apply fuzzy-logic control systems for AD optimization.

109

110 Considering the aforementioned information, the main objective of this study was to  
111 develop an advanced control system for optimizing the methane production in fixed-bed  
112 anaerobic reactors. To this purpose, a fuzzy-logic system consisting of a supervisory  
113 controller to determine the set-point of methane flow rate and an upper-layer controller to  
114 define the inflow of substrate into the reactor was first developed by simulation and then  
115 validated in a 350 L pilot-scale fixed-bed anaerobic reactor treating industrial winery  
116 wastewater. The proposed controller aimed at maximizing bio-methane production whilst  
117 controlling the VFA concentration in the effluent. The main novelty of this study lies not only  
118 in developing a controller for optimizing the operation of fixed-bed anaerobic reactors, but

119 also in its validation under specific conditions that were similar to those found in full-scale  
120 plants.

121

## 122 **2. Materials and methods**

123

### 124 *2.1. Pilot plant description and operation*

125

126 Figure 1 shows the flow diagram and the instrumentation of the continuous fixed-bed  
127 anaerobic reactor used in this study. The plant had a total volume of 358 L. The support media  
128 (Cloisonyl:  $180 \text{ m}^2 \text{ m}^{-3}$  specific surface) filled 34 L, leaving 324 L as effective volume. The  
129 anaerobic reactor was jacketed and connected to a water heating system for temperature  
130 control. Moreover, the plant was equipped with a pH control by feeding NaOH (30 %) to the  
131 system when necessary. The pH set-point was set at 7.2.

132

133 The plant was fed with industrial winery wastewater from local cellars located in the area  
134 of Narbonne, France. Table 1 shows the main average characteristics of the influent  
135 wastewater during the experimental period. The wastewater was stored in a feeding tank of 27  
136  $\text{m}^3$  that was connected to a dilution system of  $0.2 \text{ m}^3$ . The main aim of this dilution system  
137 was to allow testing different organic loading rates (OLRs) in the plant. In the reactor, a  
138 portion of the mixed liquor was recycled from the bottom to the top for both improving the  
139 mixing conditions and favouring the stripping of the produced gases from the liquid phase.  
140 The influent wastewater was mixed with the recycled mixed liquor and then introduced at the  
141 top of the reactor. The recycling flow rate was controlled manually at approximately  $550 \text{ L h}^{-1}$ .  
142 The pilot plant was operated at a controlled temperature of  $35 \text{ }^\circ\text{C}$ .

143

## 144 2.2. Pilot plant instrumentation, automation and control

145

146 As shown in Figure 1, the plant was fully automated and instrumented. The on-line  
147 equipment consisted of: one pH transmitter and one conductivity-temperature transmitter  
148 located in the recycling pipe; one temperature transmitter in the anaerobic reactor; one gas  
149 pressure transmitter in the head-space of the anaerobic reactor; two flow-rate transmitters (one  
150 for the recycling pump and one for the feed pump); one gas flow-rate transmitter  
151 (electromagnetic floater-based sensor) and one on-line CH<sub>4</sub>/CO<sub>2</sub> sensor (Ultramat 22P  
152 Siemens), both located in the biogas discharge pipeline; and one on-line titrimetric sensor  
153 (Anaerobic Control Analyser AnaSense<sup>®</sup>, AppliTek S.L.) for the measurement of total VFA  
154 and alkalinity in the reactor. On the other hand, a linear relationship ( $R^2$  above 0.8) was  
155 observed between the experimentally determined COD concentration in the effluent and the  
156 VFA measurement from the on-line titrimetric sensor. Therefore, besides its experimental  
157 determination, the COD concentration in the effluent was also predicted in real time from the  
158 continuously on-line monitored VFA concentration.

159

160 The plant also included several lower-layer control loops, which consisted of classical  
161 PIDs and on-off controllers, in order to control the influent flow rate, the temperature, and the  
162 pH. The on-line sensors and the automatic equipment were connected to a network system  
163 that included several transmitters, an input/output device, and a PC that was in charge of the  
164 data acquisition and allowed performing multi-parameter control. The input/output device was  
165 managed by a software developed at INRA-LBE. The main aim of this software was to carry  
166 out data logging, advanced control action calculations and process supervision by using  
167 Matlab<sup>®</sup> routines.

168

169 *2.3. Sampling and off-line measurements*

170

171 Besides the on-line process monitoring, samples from influent, effluent and biogas  
172 streams were collected once per day. From both influent and effluent, the chemical oxygen  
173 demand (COD) was determined twice/three times a week, whilst the composition of VFAs,  
174 *i.e.* acetate (C2), propionate (C3), iso-butyrate and butyrate (iC4 and C4), and iso-valerate and  
175 valerate (iC5 and C5), were analyzed once per day. Biogas composition (CH<sub>4</sub>, CO<sub>2</sub>, O<sub>2</sub>, H<sub>2</sub>S,  
176 and N<sub>2</sub>) was determined three times a week.

177

178 The COD was determined by the spectrophotometric micro-method (Tube Test MR,  
179 AQUALYTIC<sup>®</sup>), according to Standard Methods [31]. The composition of VFAs was  
180 determined by liquid chromatography (Perkin Elmer<sup>®</sup>, Clarus 580 Liquid Chromatograph).  
181 0.5 mL of sample was introduced into a vial with the same amount of standard (1 g of ethyl-2-  
182 butiric acid in 1 L of distilled water, acidified to 5 % (v/v) with H<sub>3</sub>PO<sub>4</sub>). Moreover, a control  
183 solution containing the VFAs to be determined (1.078 g C2 L<sup>-1</sup>; 1.022 g C3 L<sup>-1</sup>; 1.068 g iC4  
184 L<sup>-1</sup>; 1.111 g C4 L<sup>-1</sup>; 1.079 g iC5 L<sup>-1</sup>; and 1.151 g C5 L<sup>-1</sup>) was also analysed. The composition  
185 of gas was measured using a gas chromatograph equipped with a thermic conductivity  
186 detector (GC-TCD, Perkin Elmer<sup>®</sup>, Clarus 480 Gas Chromatograph). 0.2 mL of biogas were  
187 collected by a gas-tight syringe and injected into the GC, which was maintained at  
188 temperature of 65 °C and pressure of 2.48 bars. The GC consisted of two columns: one  
189 RtUBond (30m x 0.32mm x 10µm) allowing the separation of CO<sub>2</sub> and H<sub>2</sub>S; and one Rt-  
190 Molvieve 5A (30m x 0.32mm x 30µm) allowing the separation of the H<sub>2</sub>, O<sub>2</sub>, N<sub>2</sub> and CH<sub>4</sub>.  
191 The carrier gas was helium at a flow-rate of 4 mL min<sup>-1</sup>.

192

193 *2.4. Control system description*

194

195 Figure 2 shows a block diagram of the proposed fuzzy-logic controller for optimization  
196 of the performance of a fixed-bed anaerobic reactor. For that purpose the controller aimed at  
197 maximizing the bio-methane production whilst controlling the VFA content in the effluent.  
198 The proposed control structure consisted of: (i) an upper-layer controller that manipulated the  
199 influent liquid flow to maintain the methane gas flow rate close to a given set-point; and (ii) a  
200 supervisory controller that maximized the set-point of the methane flow rate to be controlled  
201 by the upper-layer controller.

202

203 The methane flow was calculated by means of the methane concentration in the gas  
204 phase and the measured biogas flow. The methane flow was corrected to account for the  
205 dependence of the biogas density on the volumetric flow. Thus, taking into account the on-  
206 line information from the biogas composition (% CH<sub>4</sub> and % CO<sub>2</sub>) and the measured biogas  
207 flow ( $G_{MEASURED}$ ), the methane flow ( $q_{CH_4}$ ) was calculated by Equation 1.

208

$$209 \quad q_{CH_4} = G_{CORRECTED} \cdot \frac{\%CH_4}{100} \quad (\text{Eq. 1})$$

210 where:

$$211 \quad - \quad G_{CORRECTED} = G_{MEASURED} \cdot frho \quad (\text{Eq. 2})$$

$$212 \quad - \quad frho = \sqrt{\frac{rho_{AIR}}{(rho_{CH_4} \cdot \%CH_4 + rho_{CO_2} \cdot \%CO_2 + rho_{N_2} \cdot (100 - \%CH_4 - \%CO_2)) / 100}} \quad (\text{Eq. 3})$$

213 -  $rho_{AIR}$ : volumetric weight of air (1.2930 kg m<sup>-3</sup>),

214 -  $rho_{CH_4}$ : volumetric weight of CH<sub>4</sub> (0.7168 kg m<sup>-3</sup>),

215 -  $rho_{CO_2}$ : volumetric weight of CO<sub>2</sub> (1.9768 kg m<sup>-3</sup>),

216 -  $rho_{N_2}$ : volumetric weight of N<sub>2</sub> (1.2505 kg m<sup>-3</sup>).

217

218 A 2h-moving average value for  $q_{CH_4}$  ( $q_{CH_4}^*$ ) was applied to the raw data to reduce the  
219 noise from the measurements. Similarly, a 2h-moving average value ( $VFA^*$ ) was also  
220 considered for the effluent VFA concentration to take into account the sampling time of the  
221 on-line titrimetric sensor. Both moving average values were also selected on the basis of AD  
222 process dynamics through experimental observations. The control time of the upper-layer  
223 controller was set to 5 h and the control time of the supervisory controller was set to 24 h. The  
224 fuzzy-logic controller was defined following the Takagi-Sugeno structure.

225

#### 226 2.4.1. Upper-layer controller description

227

228 The upper-layer controller determined the variation in the set-point of the influent flow  
229 rate ( $\Delta q_{IN\_SP}$ ) to be applied to the corresponding PID controller on the basis of three inputs:  
230 the error in the methane flow rate ( $eq_{CH_4}$ ; Equation 4), the variation in the error of the  
231 methane flow rate ( $\Delta eq_{CH_4}$ ; Equation 5) and the difference between a maximum VFA  
232 concentration ( $VFA_{MAX}$ ) and the VFA content in the effluent ( $dVFA$ ; Equation 6).

233

$$234 \quad eq_{CH_4}(t) = q_{CH_4}(t) - q_{CH_4\_SP}(t) \quad (\text{Eq. 4})$$

235 where:

236 -  $eq_{CH_4}(t)$  : error in the methane flow rate at a given time  $t$ ,

237 -  $q_{CH_4}(t)$  : measured methane flow rate at a given time  $t$ ,

238 -  $q_{CH_4\_SP}(t)$  : methane flow rate set-point at a given time  $t$ .

239

240  $\Delta eq_{CH_4}(t) = |eq_{CH_4}(t)| - \delta \cdot |eq_{CH_4}(t-1)|$  (Eq. 5)

241 where:

242 -  $\Delta eq_{CH_4}(t)$ : variation in the error of the methane flow rate at a given time  $t$ ,

243 -  $|eq_{CH_4}(t)|$ : absolute value of the error in the methane flow rate at a given time  $t$ ,

244 -  $\delta$ : modifying algebraic factor (Equation 7),

245 -  $|eq_{CH_4}(t-1)|$ : absolute value of the error in the methane flow rate at the previous

246 control action.

247

248  $dVFA(t) = VFA_{MAX} - VFA(t)$  (Eq. 6)

249 where:

250 -  $dVFA(t)$ : difference between  $VFA_{MAX}$  and the VFA content in the effluent at a given  
251 time  $t$ ,

252 -  $VFA(t)$ : effluent VFA concentration at a given time  $t$ ,

253 -  $VFA_{MAX}$ : maximum effluent VFA concentration.

254

255  $\Delta eq_{CH_4}$  is negative or positive depending on whether  $eq_{CH_4}(t)$  tends to zero or not,

256 respectively. Moreover, this equation features a modifying algebraic factor ( $\delta$ ) that is defined

257 by Equation 7 to account for opposite signs between  $|eq_{CH_4}(t)|$  and  $|eq_{CH_4}(t-1)|$ .

258

259  $\delta = \frac{eq_{CH_4}(t) \cdot eq_{CH_4}(t-1)}{|eq_{CH_4}(t) \cdot eq_{CH_4}(t-1)|}$  (Eq. 7)

260



261 For the fuzzification stage, three Gaussian membership functions, represented by  
 262 Equation 8, were considered for  $eq_{CH_4}$  and  $\Delta eq_{CH_4}$ : Negative (*N*), Zero (*Z*) and Positive (*P*);  
 263 and one Gaussian membership function was defined for *dVFA*: Zero (*Z*). As each Gaussian  
 264 membership function is defined by two parameters (centre *c* and amplitude *a*), the control  
 265 system had a total of 14 parameters as regards to the fuzzification stage. Concerning the  
 266 defuzzification stage, four singleton membership functions were defined for  $\Delta q_{IN\_SP}$ : High  
 267 Negative (*HN*), Low Negative (*LN*), Low Positive (*LP*) and High Positive (*HP*). Therefore,  
 268 the control system had a total of 4 parameters regarding the defuzzification stage.

269

$$270 \quad \mu(p) = \exp\left(-\frac{(p-c)^2}{2\sigma^2}\right) \quad (\text{Eq. 8})$$

271 where:

- 272 -  $\mu(p)$ : degree of membership of the input variable *p*,
- 273 - *p*: numerical value of the variable,
- 274 - *c*: centre of the Gaussian-type membership function,
- 275 -  $\sigma$ : amplitude of the Gaussian-type membership function.

276

277 Table 2 shows the resulting grade of membership to the different output linguistic labels  
 278 that define the output fuzzy set. As this table shows, the effect of the input variable *dVFA*  
 279 (represented by the third right-side term of rules #1, #2, #5a and #6b, *i.e.*  $1 - \mu(dVFA)_Z$ ) on  
 280 the output linguistic variable decreases as the effluent VFA concentration decreases (*i.e.* if  $\mu$   
 281  $(dVFA)_Z = 0$  then  $1 - \mu(dVFA)_Z = 1$ ). On the contrary, the effect of *dVFA* cancels the  
 282 corresponding control action when the effluent VFA concentration is close to  $VFA_{MAX}$  (*i.e.* if  
 283  $\mu(dVFA)_Z = 1$  then  $1 - \mu(dVFA)_Z = 0$ ). Hence, the increase in the influent flow rate

284 controlled by the inference rules #1, #2, #5a and #6b is cancelled when the system is working  
285 at maximum VFA capacity.

286

287 The output linguistic variable ( $\Delta q_{IN\_SP}$ ) was obtained by applying Larsen's fuzzy  
288 inference method [32]. In the defuzzification stage, the Height Defuzzifier method was  
289 employed [33] to obtain a single output value from the output fuzzy set.

290

291 Finally, the control action of the upper-layer controller was calculated as expressed by  
292 Equation 9.

293

$$294 \quad q_{IN\_SP}(t) = q_{IN\_SP}(t-1) + \Delta q_{IN\_SP}(t) \quad (\text{Eq. 9})$$

295

#### 296 2.4.2. Supervisory controller description

297

298 The supervisory controller determined the variation in the set-point of the methane flow  
299 rate ( $\Delta q_{CH_4\_SP}$ ) on the basis of two inputs: the error in the methane flow rate (Equation 4) and  
300 the accumulated error in the methane flow rate (Equation 10).

301

$$302 \quad \Sigma eq_{CH_4}(t) = \Sigma eq_{CH_4}(t-1) + ST \cdot eq_{CH_4}(t) \quad (\text{Eq. 10})$$

303 where:

- 304 -  $\Sigma eq_{CH_4}(t)$ : accumulated error in the methane flow rate at a given time,
- 305 -  $\Sigma eq_{CH_4}(t-1)$ : accumulated error in the methane flow rate at the previous sampling  
306 time ( $ST$ ),

307

308 Regarding the fuzzification stage, three additional Gaussian membership functions were  
309 considered for  $\Sigma eq_{CH_4}$  : Negative (*N*), Zero (*Z*) and Positive (*P*). Concerning the  
310 defuzzification stage, three singleton membership functions were defined for  $\Delta q_{CH_4\_SP}$  : Low  
311 Negative (*LN*), Low Positive (*LP*) and High Positive (*HP*). Thus, the supervisory controller  
312 added to the proposed fuzzy-logic controller a total of 6 and 3 parameters regarding  
313 fuzzification and defuzzification, respectively. Table 2 shows the resulting grade of  
314 membership to the different output linguistic labels that defined the output fuzzy set of the  
315 supervisory controller.

316

317 The output linguistic variable ( $\Delta q_{CH_4\_SP}$ ) was determined following the method described  
318 in section 2.4.2. Finally, the control action of the supervisory controller was calculated as  
319 expressed by Equation 11.

320

$$321 \quad q_{CH_4\_SP}(t) = q_{CH_4\_SP}(t-1) + \Delta q_{CH_4\_SP}(t) \quad (\text{Eq. 11})$$

322

### 323 *2.4.3. Simulation-based design and validation*

324

325 The controller was firstly designed and tuned by simulation in Matlab<sup>®</sup> Simulink<sup>®</sup> using  
326 the Fuzzy Logic Toolbox<sup>™</sup>. To this aim, a simplified version of the model BNRM2 [34] was  
327 used. This model considers the main physicochemical and biological processes taking place  
328 during AD, including gas-liquid transfer (nitrogen, ammonia, oxygen, hydrogen, methane and  
329 carbon dioxide), a chemical model for pH calculation and biological steps such as  
330 acidogenesis, acetogenesis and acetoclastic and hydrogenotrophic methanogenesis. Therefore,  
331 this model allowed the simulation of the methane production rates and the concentrations of

332 VFAs in the effluent.

333

334 The control tuning was performed by a trial-error approach until obtaining an adequate  
335 response (*i.e.* a deviation of less than 5 % between the response and the set-point given by the  
336 supervisory controller).

337

### 338 **3. Results and discussion**

339

#### 340 *3.1. Simulation-based validation of the control system*

341

342 Figure 3 shows the performance of the advanced controller obtained by simulation after  
343 control tuning. Figure 3a presents the evolution of the resulting methane flow rate and the  
344 corresponding set-point commanded by the supervisory controller, and the influent flow rate  
345 commanded by the upper-layer controller. Figure 3b shows the effluent VFA concentration  
346 and the  $VFA_{MAX}$  considered.  $VFA_{MAX}$  was set to 750 mg COD L<sup>-1</sup> (value fixed from knowledge  
347 obtained from previous experiments). This maximum VFA concentration resulted in a  
348 minimum COD removal efficiency of 80%.

349

350 It must be mentioned that the value of  $VFA_{MAX}$  has to be carefully selected according to  
351 the control objectives (*i.e.* enhance AD performance and stability, minimize VFA contents in  
352 the effluent, meet COD discharge limits, achieve VFA requirements in downstream  
353 processes...) and process specificities. For instance, higher  $VFA_{MAX}$  values can be potentially  
354 applied without risk of reactor acidification if the controller performs in a high-alkalinity  
355 system. On the other hand, lower  $VFA_{MAX}$  values should be applied when the alkalinity of the  
356 system is low or when no pH control is possible, thus reducing the propensity of possible

357 acidification problems.

358

359 As Figure 3a shows, the controller was able to maintain the simulated methane flow at  
360 values close to the controlled set-point until reaching the constraint of the maximum VFA  
361 concentration ( $750 \text{ mg COD L}^{-1}$ ). This maximum VFA concentration was approached from  
362 days 5 to 6, thus the increase in the influent flow rate was almost null. Only when the VFA  
363 concentration was below its maximum threshold value it was possible to increase slightly the  
364 influent flow rate to compensate the negative error in the methane flow (see period from day 6  
365 to end). As the differences between the measured and the desired values were getting smaller,  
366 also did the changes in  $q_{CH_4\_SP}$  and  $q_{IN\_SP}$ . Within an infinite time and no external  
367 disturbances, the concentrations of VFA would eventually reach  $VFA_{MAX}$ , showing an optimal  
368 performance according to the desired VFA content in the effluent.

369

370 It is important to notice that during the first period of simulation, when the VFA  
371 concentrations were low, the methane production was higher than the one commanded by the  
372 supervisory controller (*e.g.* 2<sup>nd</sup> day). However, the supervisory controller did not increase  
373 more the set-point in order to avoid overloading the reactor.

374

### 375 3.2. *Experimental validation of the control system*

376

377 Figure 4 presents the evolution of the OLR and HRT throughout the experimental period.  
378 As it can be observed, the operational period is divided in 3 different sections: (I) reactor  
379 start-up; (II) transitory period including a pH-shock due to failure of the pH sensor; and (III)  
380 controlled process. As Figure 4 shows, the OLR was manually increased from 0 to  $4 \text{ g COD}$   
381  $\text{L}^{-1} \text{ d}^{-1}$  from day 0 to around 40, whilst maintaining the HRT around 3 d. This progressive

382 increase in the OLR was carried out to minimize possible disturbances during the biofilm  
383 formation at the start-up process. During this period, the concentration of VFAs in the effluent  
384 was used as state indicator of the process performance. This allowed avoiding the inhibition  
385 of the newly-grown biomass due to overloading of the reactor. This is the reason for the  
386 decrease in the OLR from days 20 to 30. During this period, high VFA concentrations were  
387 observed in the effluent (up to 1500 mg COD L<sup>-1</sup>) and, as the acetate inhibition coefficient of  
388 propionic-oxidizing bacteria is around 2500 mg COD L<sup>-1</sup> (see, for instance, Siegert and Banks  
389 [35]), the OLR was reduced to avoid inhibition of these microorganisms. Around day 50  
390 (period II in Figure 4), a significant increase of the pH in the reactor (up to around 9) occurred  
391 due to a failure in the lower-layer pH controller (data not shown). This resulted in a  
392 considerable decay of the anaerobic biomass. Therefore, the OLR and HRT were set to 1.4 g  
393 COD L<sup>-1</sup> d<sup>-1</sup> and 9 d, respectively, in order to recover the system to appropriate operating  
394 conditions. From day 61 on (period III in Figure 4), the advanced controller was turned on for  
395 optimizing the process performance. Figure 4 shows that the controller increased  
396 progressively the inflow to the reactor until reaching the maximum treatment capacity of the  
397 system, which was limited by  $VFA_{MAX}$  (set at 750 mg COD L<sup>-1</sup>).

398

399 Figure 5 shows the evolution throughout the operational period of: the methane yield  
400 (Figure 5a); and the total COD removed in the system and the COD fraction removed for  
401 methane production (Figure 5b). As Figure 5 shows, no methane production was observed  
402 until day 20. This suggests that the removal of COD from days 10 to 20 was mainly related to  
403 the anabolism of the anaerobic biomass (*i.e.* initial growth, fixation, and acclimation of the  
404 biomass [7]) and to the production of the gas required for filling the headspace volume of the  
405 reactor and to achieve conditions of gas-liquid equilibrium within the system. Therefore, 20  
406 days was identified in this study as the minimum time for obtaining a functional anaerobic

407 biomass consortium under conditions of equilibrium. The decrease in the COD removal  
408 observed from days 25 to 30 was related to the aforementioned accumulation of VFAs. After  
409 decreasing the OLR, the COD removal efficiency was restored. From day 30 to around 50, a  
410 quite stable COD removal efficiency (up to 85 %) was achieved. Concerning to the methane  
411 yields after day 20, this value increased greatly (reaching values up to 0.34 L<sub>CH<sub>4</sub></sub> per gram of  
412 COD removed) due to catabolism of methanogenic archaea. However, this value decreased  
413 from 0.32 to 0.10 L<sub>CH<sub>4</sub></sub> g<sup>-1</sup> COD<sub>REM</sub> from day 25 to day 30. According to Michaud et al. [7],  
414 this may have been caused by disturbances occurring during the initial contact of the  
415 microorganisms and the fixed support media. Therefore, even it after 20 days a functional  
416 anaerobic biomass existed, a minimum time of 35 days was needed to obtain a functional  
417 anaerobic biofilm. This value is in agreement with previous results reported in the literature  
418 (see, for instance, Michaud et al. [7]). Afterwards, the methane yield increased continuously  
419 throughout this operational period (except for period II), reaching again values up to 0.34  
420 L<sub>CH<sub>4</sub></sub> g<sup>-1</sup> COD<sub>REM</sub>. This behaviour suggested the development and maturing of a stable  
421 biofilm.

422

423 As mentioned before, during period II a system failure occurred due to a pH-shock. As  
424 Figure 5 illustrates, both COD removal for methane production and methane yield presented a  
425 sharp decrease. Nevertheless, when the control system was turned back on (period III), it was  
426 possible to quickly recover the system to the previous state, achieving values of methane  
427 yields and COD removals for methane production of around 0.34 L<sub>CH<sub>4</sub></sub> g<sup>-1</sup> COD<sub>REM</sub> and 85 %,   
428 respectively.

429

430 The fixed-bed anaerobic reactor achieved an efficient and stable performance when  
431 running the proposed advanced controller (period III). As Figure 5b shows, COD removal

432 efficiencies above 80 % were achieved during this period. In addition, a high stable methane  
433 yield of around  $0.34 \text{ L}_{\text{CH}_4} \text{ g}^{-1} \text{ COD}_{\text{REM}}$  was reached (see Figure 5a). These results highlighted  
434 the suitable performance of the process under controlled conditions. Indeed, comparing the  
435 results from periods I and III, it can be stated that enhanced process performances were  
436 achieved in terms of COD removal, methane production and treatment capacity.

437

438 Figure 6 shows the performance of the advanced controller during the operational period  
439 III. As it can be observed, the supervisory controller increased continuously the set-point for  
440 the methane flow rate (see Figure 6a) until reaching the maximum effluent VFA concentration  
441 (see Figure 6b). Therefore, the upper-layer controller continuously increased the influent flow  
442 to reach the corresponding methane flow rate set-point. As a result, a maximum methane  
443 production of around  $17 \text{ L h}^{-1}$  was reached when operating with a  $VFA_{\text{MAX}}$  of  $750 \text{ mg COD L}^{-1}$ .  
444 A deviation of the methane flow rate from the established set-point lower than 10 % was  
445 achieved, whilst the methane yield was maintained around  $0.35 \text{ L}_{\text{CH}_4} \text{ g}^{-1} \text{ COD}$  during the  
446 pseudo-stationary operational period (see days 65 to the end in Figure 5a). Throughout this  
447 period, a methane-rich biogas was also produced (with methane contents in the biogas around  
448  $85 \pm 2 \%$ ).

449

450 As designed, the controller increased  $q_{\text{CH}_4\_SP}$  only if the concentration of VFA in the  
451 effluent was below  $VFA_{\text{MAX}}$ . The results from days 70 to 73 show that, even if  $eq_{\text{CH}_4}$  was  
452 negative (*i.e.*  $q_{\text{IN\_SP}}$  could be higher), the supervisory controller did not allow increasing the  
453 influent flow rate because the concentration of VFA was over  $VFA_{\text{MAX}}$ . The same occurred the  
454 days 77-78, verifying the correct performance of the controller.

455



456 As explained in section 3.1., without disturbances the process would reach eventually  
457  $VFA_{MAX}$ , never overpassing it. However, this value was reached and overpassed in different  
458 occasions, suggesting that, as in any real process, disturbances affected the system. As the  
459 temperature and the pH were controlled and kept at barely constant values, the most likely  
460 sources of disturbances were the feed itself and the recirculation flow. Heterogeneity of the  
461 substrate may have caused small differences in the COD entering the reactor. In addition, as  
462 the substrate was kept into a feeding tank before entering the reactor, some extent of  
463 degradation had already occurred during the storage period, modifying the input concentration  
464 of VFA. Moreover, as the recirculation flow was manually controlled, there were sudden  
465 drops in the recycling flow rate due to partial clogging of the tubing. This caused significant  
466 variations of this parameter throughout the operational period (varying from 100 to 700 L h<sup>-1</sup>).  
467 This may have affected the methane production, mainly by modifying the stripping rate of the  
468 produced gases from the liquid phase. Lower recycling flow rates might cause lower methane  
469 stripping rates from the liquid phase, leading to lower gaseous outflow rates of methane.  
470 However, the control action was able to compensate the disturbances in the methane  
471 production, achieving anyway the desired set-point. Therefore, the fuzzy-logic control action  
472 resulted in a suitable performance under disturbances which are likely to be similar to those  
473 expected in full-scale plants (*e.g.* variations in the recycling flow rate).

474

475 It can be concluded that, after a relatively simple calibration, the proposed fuzzy-logic  
476 controller was able to successfully optimize the process performance, maximizing the  
477 methane production and the VFA content in the effluent up to the chosen fixed values, whilst  
478 resulting in adequate COD removal efficiencies and methane yields. At this point, it is  
479 important to mention that, as the organic matter within the winery wastewater used as  
480 substrate is mainly composed of soluble COD, the AD kinetics were not limited by the

481 hydrolysis step. This allowed the application of a short period for the evaluation of the control  
482 strategy.

483

484 Finally, when considering the application of this fuzzy-logic control system at full-scale  
485 for control and optimization, different modifications might be considered to further improve  
486 the performance, such as optimization of the control dynamics for both controllers, fine  
487 adjustment of the knowledge-based fixed values (*i.e.*,  $VFA_{MAX}$ ) and optimization of the tuning  
488 parameters (*i.e.* centre, amplitude and singleton values for the fuzzification and  
489 defuzzification stages), among others.

490

#### 491 **4. Conclusions**

492

493 A fuzzy-logic based controller for optimizing the process performance of a 350 L fixed-  
494 bed anaerobic reactor treating winery wastewater was developed by simulation and validated  
495 under specific conditions that were similar to the ones expected at full-scale plants. The  
496 controller aimed at maximizing the methane productivity whilst controlling the VFA content  
497 in the effluent. By application of the fuzzy-logic control system, a deviation of the methane  
498 flow from the established set-point lower than 10 % was achieved. The methane yield resulted  
499 in values around  $0.29 \text{ L}_{\text{CH}_4} \text{ g}^{-1} \text{ COD}$ , with COD removal efficiencies of up to 85 % obtained  
500 throughout the whole experimental period. On the other hand, the controller allowed an  
501 adequate control of the VFA content in the effluent, with values close to the established set-  
502 point ( $750 \text{ mg COD L}^{-1}$ ). Hence, the proposed fuzzy-logic controller was able to successfully  
503 control the system performance close to optimal conditions, maximizing the methane  
504 productivity and the VFA concentration, whilst resulting in adequate COD removal  
505 efficiencies and methane yields.

506

507 **Acknowledgements**

508

509 This research work has been supported by the Spanish Research Foundation (MICINN  
510 FPI grant BES-2009-023712), which is gratefully acknowledged.

511

512 **References**

513

514 [1] X.M. Guo, E. Trably, E. Latrille, H. Carrre, J.P. Steyer, Hydrogen production from  
515 agricultural waste by dark fermentation: A review, *Int. J. Hydrogen Energy*. 35 (2010)  
516 10660–10673.

517 [2] C.A. Aceves-Lara, E. Latrille, J.P. Steyer, Optimal control of hydrogen production in a  
518 continuous anaerobic fermentation bioreactor, *Int. J. Hydrogen Energy*. 35 (2010)  
519 10710–10718.

520 [3] I. Angelidaki, P. Kongjan, Biorefinery for sustainable biofuel production from energy  
521 crops; conversion of lignocellulose to bioethanol, biohydrogen and methane, in: 11th  
522 IWA World Congr. Anaerob. Dig., Brisbane, Australia, 2007.

523 [4] E. Aguilar-Garnica, D. Dochain, V. Alcaraz-González, V. González-Álvarez, A  
524 multivariable control scheme in a two-stage anaerobic digestion system described by  
525 partial differential equations, *J. Process Control*. 19 (2009) 1324–1332.

526 [5] J. Von Sachs, U. Meyer, P. Rys, H. Feitkenhauer, New approach to control the  
527 methanogenic reactor of a two-phase anaerobic digestion system, *Water Res*. 37 (2003)  
528 973–982.

529 [6] L. Lardon, A. Puñal, J.-P. Steyer, On-line diagnosis and uncertainty management using  
530 evidence theory—experimental illustration to anaerobic digestion processes, *J. Process*

- 531 Control. 14 (2004) 747–763.
- 532 [7] S. Michaud, N. Bernet, P. Buffière, M. Roustan, R. Moletta, Methane yield as a  
533 monitoring parameter for the start-up of anaerobic fixed film reactors, *Water Res.* 36  
534 (2002) 1385–1391.
- 535 [8] A. Ghouali, T. Sari, J. Harmand, Maximizing biogas production from the anaerobic  
536 digestion, *J. Process Control.* 36 (2015) 79–88.
- 537 [9] K. Boe, D.J. Batstone, J.-P. Steyer, I. Angelidaki, State indicators for monitoring the  
538 anaerobic digestion process, *Water Res.* 44 (2010) 5973–5980.  
539 <http://dx.doi.org/10.1016/j.watres.2010.07.043>.
- 540 [10] J.P. Steyer, J.C. Bouvier, T. Conte, P. Gras, J. Harmand, J.P. Delgenes, On-line  
541 measurements of COD, TOC, VFA, total and partial alkalinity in anaerobic digestion  
542 processes using infra-red spectrometry, *Water Sci. Technol.* 45 (2002) 133–138.
- 543 [11] J.P. Steyer, J.C. Bouvier, T. Conte, P. Gras, P. Sousbie, Evaluation of a four year  
544 experience with a fully instrumented anaerobic digestion process, *Water Sci. Technol.*  
545 45 (2002) 495–502.
- 546 [12] C. Charnier, E. Latrille, L. Lardon, J. Miroux, J.P. Steyer, Combining pH and electrical  
547 conductivity measurements to improve titrimetric methods to determine ammonia  
548 nitrogen, volatile fatty acids and inorganic carbon concentrations, *Water Res.* 95 (2016)  
549 268–279.
- 550 [13] A.D. Kalafatis, L. Wang, W.R. Cluett, Linearizing feedforward-feedback control of pH  
551 processes based on the Wiener model, *J. Process Control.* 15 (2005) 103–112.
- 552 [14] A. Schaum, J. Alvarez, J.P. Garcia-Sandoval, V.M. Gonzalez-Alvarez, On the  
553 dynamics and control of a class of continuous digesters, *J. Process Control.* 34 (2015)  
554 82–96.
- 555 [15] J. Jimenez, E. Latrille, J. Harmand, A. Robles, J. Ferrer, D. Gaida, C. Wolf, F. Mairet,

- 556 O. Bernard, V. Alcaraz-Gonzalez, Instrumentation and control of anaerobic digestion  
557 processes: a review and some research challenges, *Rev. Environ. Sci. Bio/Technology*.  
558 14 (2015) 615–648.
- 559 [16] L.A. Zadeh, Fuzzy sets, *Inf. Control*. 8 (1965) 338–353.
- 560 [17] H.B. Verbruggen, P.M. Bruijn, Fuzzy control and conventional control: What is (and  
561 can be) the real contribution of Fuzzy Systems?, *Fuzzy Sets Syst.* 90 (1997) 151–160.
- 562 [18] M. V Ruano, J. Ribes, G. Sin, A. Seco, J. Ferrer, A systematic approach for fine-tuning  
563 of fuzzy controllers applied to WWTPs, *Environ. Model. Softw.* 25 (2010) 670–676.
- 564 [19] A. Robles, M.V. Ruano, J. Ribes, J. Ferrer, Advanced control system for optimal  
565 filtration in submerged anaerobic MBRs (SAnMBRs), *J. Memb. Sci.* 430 (2013) 330–  
566 341.
- 567 [20] A. Robles, M. V Ruano, J. Ribes, A. Seco, J. Ferrer, Model-based automatic tuning of a  
568 filtration control system for submerged anaerobic membrane bioreactors (AnMBR), *J.*  
569 *Memb. Sci.* 465 (2014) 14–26.
- 570 [21] G. Olsson, M.K. Nielsen, Z. Yuan, A. Lynggaard-Jensen, Instrumentation, control and  
571 automation in wastewater systems, IWA publishing, 2005.
- 572 [22] M. Estaben, M. Polit, J.P. Steyer, Fuzzy control for an anaerobic digester, *Control Eng.*  
573 *Pract.* 5 (1997) 1303–1310.
- 574 [23] A. Genovesi, J. Harmand, J.P. Steyer, A fuzzy logic based diagnosis system for the on-  
575 line supervision of an anaerobic digester pilot-plant, *Biochem. Eng. J.* 3 (1999) 171–  
576 183.
- 577 [24] O. Bernard, M. Polit, Z. Hadj-Sadok, M. Pengov, D. Dochain, M. Estaben, P. Labat,  
578 Advanced monitoring and control of anaerobic wastewater treatment plants: software  
579 sensors and controllers for an anaerobic digester, *Water Sci. Technol.* 43 (2001) 175–  
580 182.

- 581 [25] M. Polit, A. Genovesi, B. Claudet, Fuzzy logic observers for a biological wastewater  
582 treatment process, *Appl Numer Math.* 39 (2001) 173–180.
- 583 [26] Á. Robles, F. Durán, M.V. Ruano, J. Ribes, A. Rosado, A. Seco, J. Ferrer,  
584 Instrumentation, control, and automation for submerged anaerobic membrane  
585 bioreactors, *Environ. Technol.* 36 (2015) 1–12.
- 586 [27] A. Puñal, L. Palazzotto, J.C. Bouvier, T. Conte, J.P. Steyer, Automatic control of  
587 volatile fatty acids in anaerobic digestion using a fuzzy logic based approach, *Water*  
588 *Sci. Technol.* 48 (2003) 103–110.
- 589 [28] E. Murnleitner, T.M. Becker, A. Delgado, State detection and control of overloads in  
590 the anaerobic wastewater treatment using fuzzy logic, *Water Res.* 36 (2002) 201–211.
- 591 [29] A. Robles, E. Latrille, M. V. Ruano, J.P. Steyer, A fuzzy-logic-based controller for  
592 methane production in anaerobic fixed-film reactors, *Environ. Technol.* 38 (2017).
- 593 [30] S. Carlos-Hernandez, J.F. Beteau, E.N. Sanchez, Intelligent control strategy for an  
594 anaerobic fluidized bed reactor, *IFAC Proc. Vol.* 40 (2007) 73–78.
- 595 [31] APHA, *Standard Methods for the Examination of Water and Wastewater*, 21st ed.,  
596 American Public Health Association, Washington, DC, 2005.
- 597 [32] P.M. Larsen, Industrial applications of fuzzy logic control, *Int. J. Man. Mach. Stud.* 12  
598 (1980) 3–10.
- 599 [33] J.M. Mendel, Fuzzy logic systems for engineering: a tutorial, *Proc. IEEE.* 83 (1995)  
600 345–377.
- 601 [34] R. Barat, J. Serralta, M. V Ruano, E. Jiménez, J. Ribes, A. Seco, J. Ferrer, Biological  
602 Nutrient Removal Model No. 2 (BNRM2): a general model for wastewater treatment  
603 plants, *Water Sci. Technol.* 67 (2013) 1481–1489.
- 604 [35] I. Siegert, C. Banks, The effect of volatile fatty acid additions on the anaerobic  
605 digestion of cellulose and glucose in batch reactors, *Process Biochem.* 40 (2005) 3412–

606 3418.

607

608 **Figure and table captions**

609 **Figure 1.** Flow diagram of the plant, including instrumentation. (Nomenclature: **FIT**: Flow-  
610 Indicator-Transmitter; **PIT**: Pressure-Indicator-Transmitter; **pH**: pH-Transmitter; **CT**:  
611 Conductivity-Transmitter; **T**: Temperature sensor; **PLC**: Programmable Logic Controller).

612 **Figure 2.** Flow diagram of the advanced fuzzy-logic controller

613 **Figure 3.** Simulation of the control system performance. Evolution of: **(a)** methane flow and  
614 influent flow; and **(b)** VFA content in the effluent

615 **Figure 4.** Evolution during the operational period of OLR and HRT. (I), (II) and (III) stand  
616 for the different sections of the operational period

617 **Figure 5.** Evolution during the operational period of: (a) methane yield; and (b) fraction of  
618 total COD removed and fraction of COD removed for methane production. (I), (II) and (III)  
619 stand for the different sections of the operational period

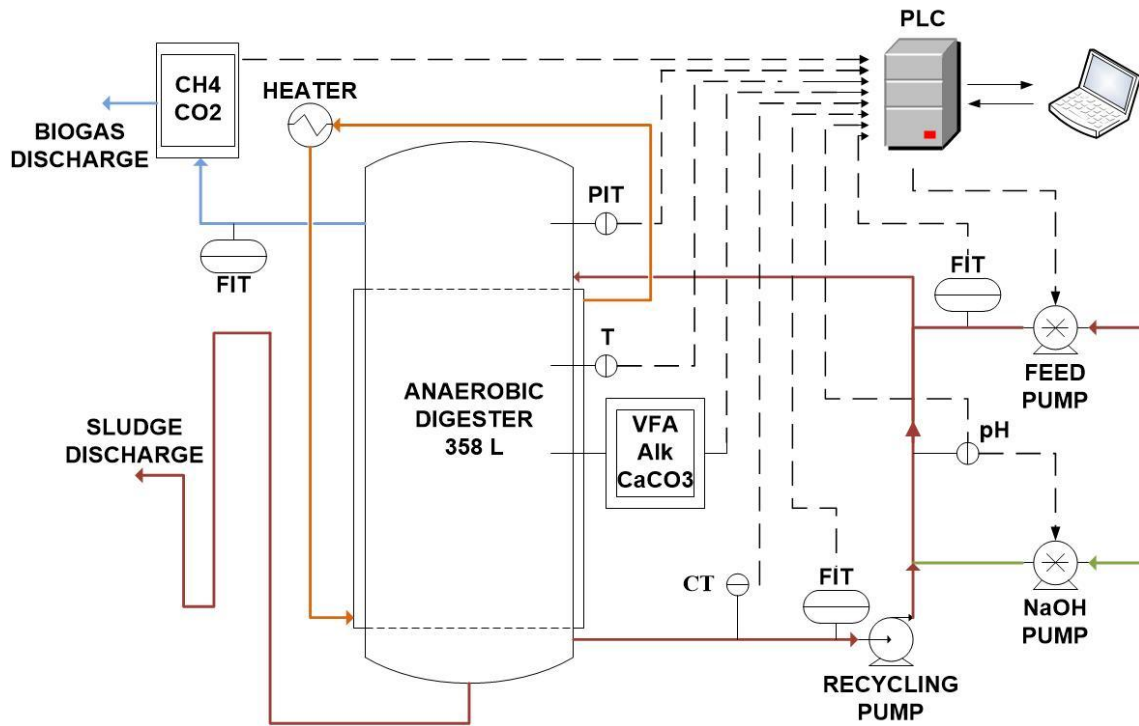
620 **Figure 6.** Control system performance. Evolution of: (a) methane flow and influent flow; and  
621 (b) VFA content in the effluent. SP stands for Set-points. The values marked with \* represent  
622 the 2h-moving averages of the measured values (every 60 min)

623

624 **Table 1.** Average raw wastewater characteristics

625 **Table 2.** Advanced fuzzy-logic controller action: grade of membership to the output linguistic  
626 labels



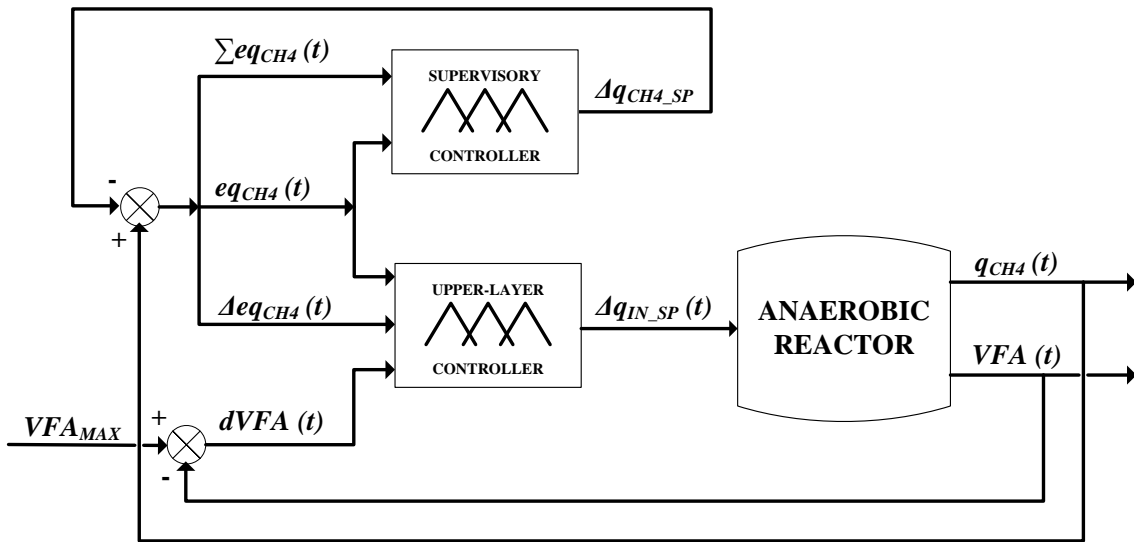


627

628 **Figure 1.** Flow diagram of the plant, including instrumentation. (Nomenclature: **FIT**: Flow-

629 Indicator-Transmitter; **PIT**: Pressure-Indicator-Transmitter; **pH**: pH-Transmitter; **CT**:

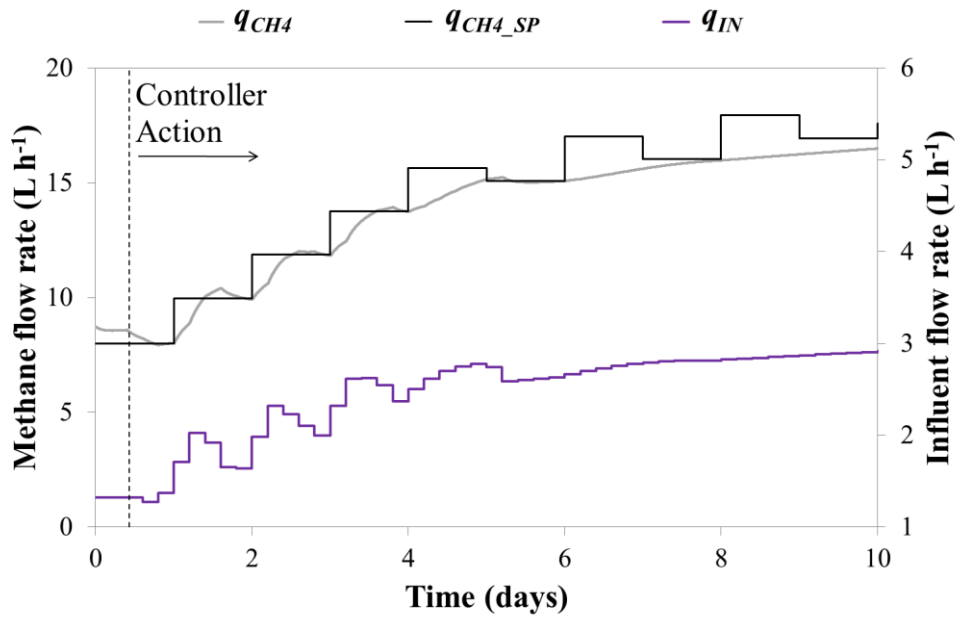
630 Conductivity-Transmitter; **T**: Temperature sensor; **PLC**: Programmable Logic Controller)



631

632

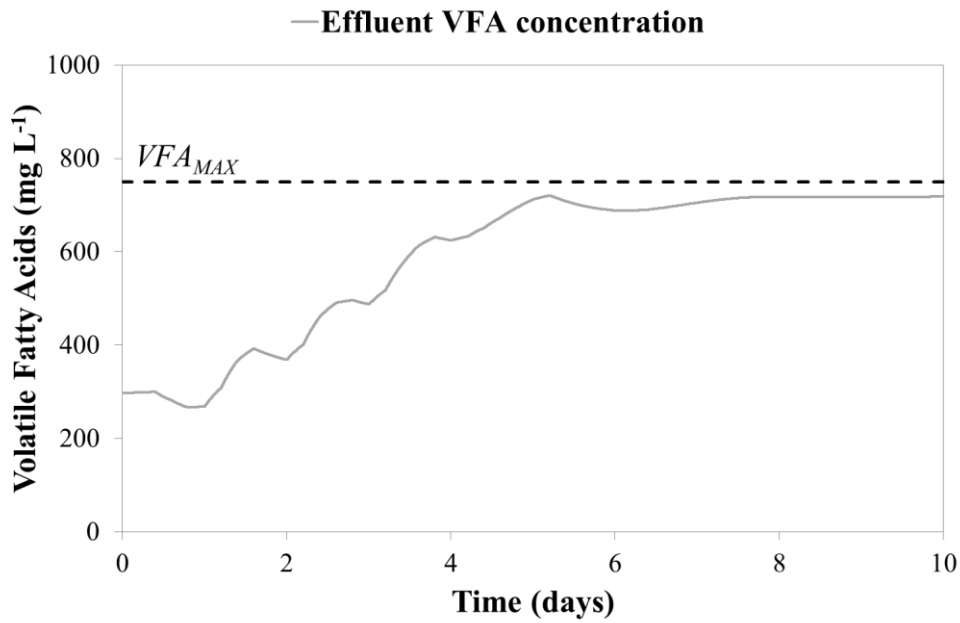
**Figure 2.** Flow diagram of the advanced fuzzy-logic controller



633

634

(a)



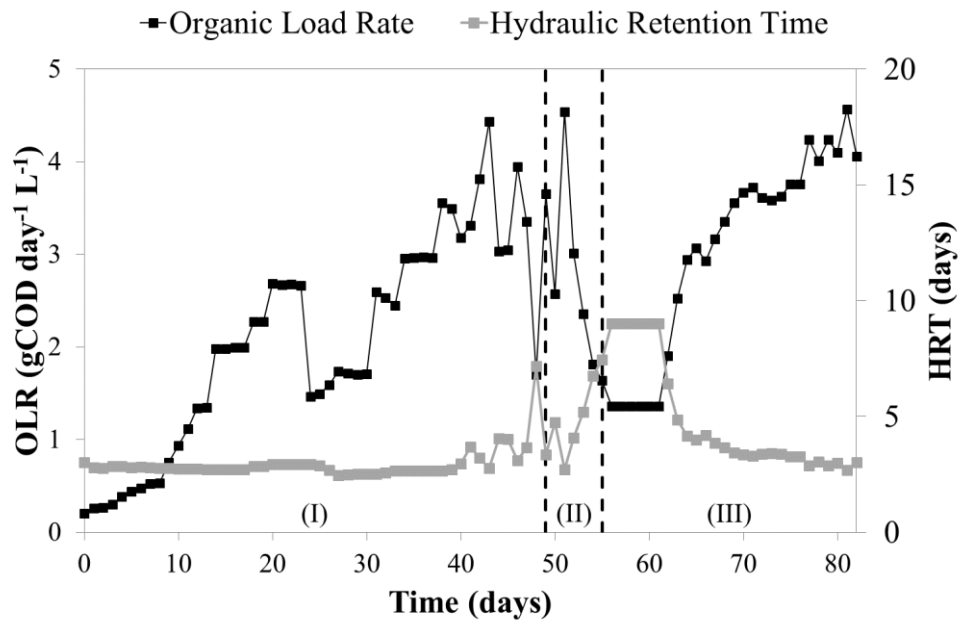
635

636

(b)

637 **Figure 3.** Simulation of the control system performance. Evolution of: (a) methane flow and

638 influent flow; and (b) VFA content in the effluent

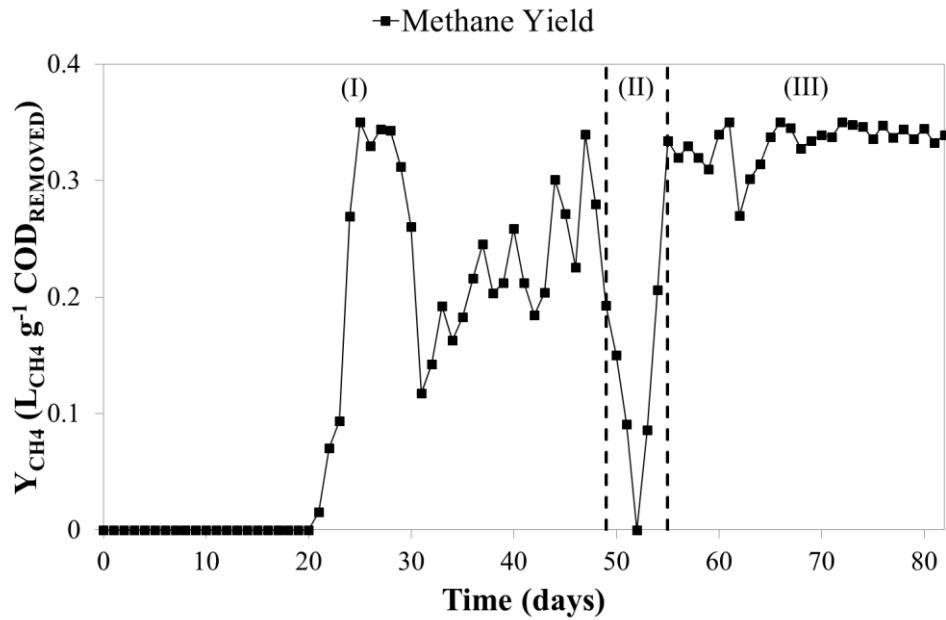


639

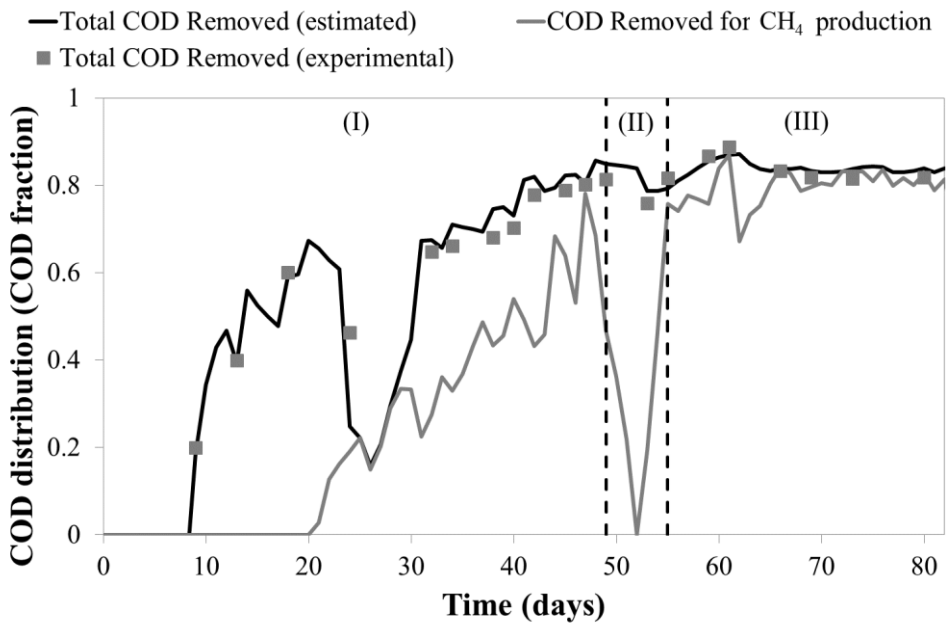
640 **Figure 4.** Evolution during the operational period of OLR and HRT. (I), (II) and (III) stand

641

for the different sections of the operational period

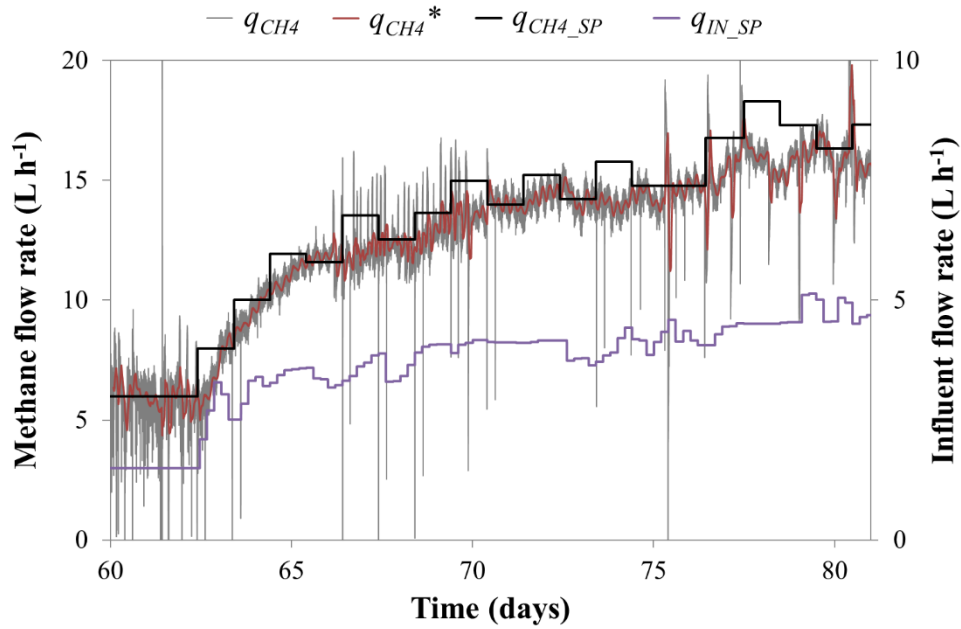


(a)



(b)

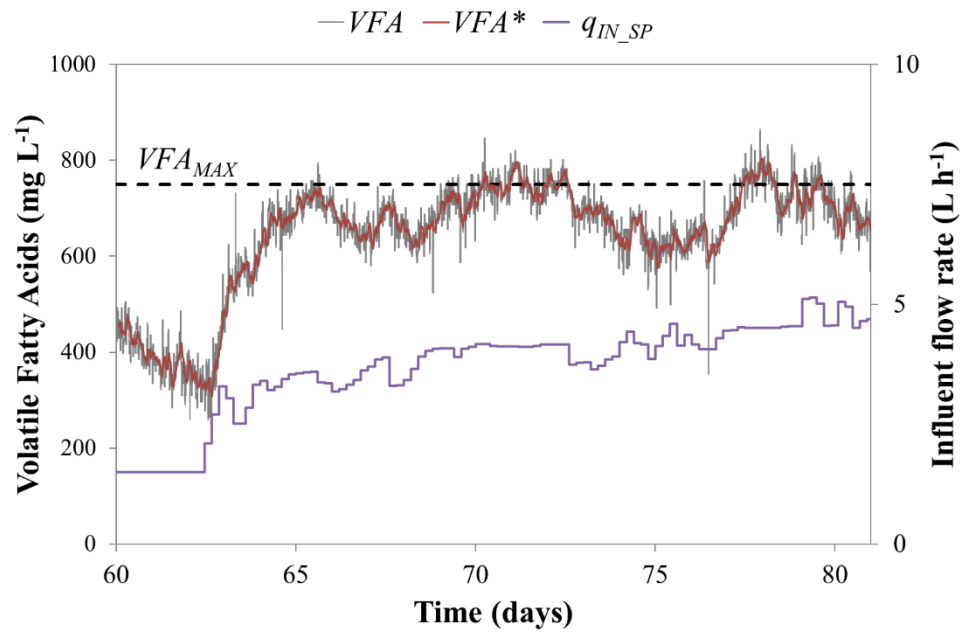
**Figure 5.** Evolution during the operational period of: (a) methane yield; and (b) fraction of total COD removed and fraction of COD removed for methane production. (I), (II) and (III) stand for the different sections of the operational period



649

650

(a)



651

652

(b)

653 **Figure 6.** Control system performance. Evolution of: (a) methane flow and influent flow; and

654 (b) VFA content in the effluent. SP stands for Set-points. The values marked with \* represent

655 the 2h-moving averages of the measured values (every 60 min)

656 **Table 1.** Average raw wastewater characteristics

<b>Parameter</b>	<b>Unit</b>	<b>Mean <math>\pm</math> SD</b>
COD	g COD L <sup>-1</sup>	21.6 $\pm$ 0.8
Acetate	g COD L <sup>-1</sup>	3.7 $\pm$ 0.4
Propionate	g COD L <sup>-1</sup>	4.6 $\pm$ 0.8
Butyrate	g COD L <sup>-1</sup>	2.8 $\pm$ 0.3
Valerate	g COD L <sup>-1</sup>	1.5 $\pm$ 0.7

657

658 **Table 2.** Advanced fuzzy-logic controller action: grade of membership to the output linguistic  
659 labels

Inference Rule	Grade of membership to the output linguistic variables				
<i>Supervisory controller</i>					
A	$\mu (\Delta q_{CH_4\_SP})_{HP}$	=	$\mu (eq_{CH_4})_Z$	·	$\mu (\Sigma eq_{CH_4})_Z$
B	$\mu (\Delta q_{CH_4\_SP})_{LN}$	=	$\mu (eq_{CH_4})_N$	·	$\mu (\Sigma eq_{CH_4})_N$
C	$\mu (\Delta q_{CH_4\_SP})_{LP}$	=	$\mu (eq_{CH_4})_P$	·	$\mu (\Sigma eq_{CH_4})_P$
<i>Upper-layer controller</i> <span style="float: right;">* <math>eq_{CH_4} &lt; 0</math>; ** <math>eq_{CH_4} &gt; 0</math></span>					
1	$\mu (\Delta q_{IN})_{HP}$	=	$\mu (eq_{CH_4})_N$	·	$\mu (\Delta eq_{CH_4})_Z \cdot (1 - \mu (dVFA)_Z)$
2	$\mu (\Delta q_{IN})_{HP}$	=	$\mu (eq_{CH_4})_N$	·	$\mu (\Delta eq_{CH_4})_P \cdot (1 - \mu (dVFA)_Z)$
3	$\mu (\Delta q_{IN})_{HN}$	=	$\mu (eq_{CH_4})_P$	·	$\mu (\Delta eq_{CH_4})_Z$
4	$\mu (\Delta q_{IN})_{HN}$	=	$\mu (eq_{CH_4})_P$	·	$\mu (\Delta eq_{CH_4})_P$
5*	$\mu (\Delta q_{IN})_{LP}$	=	$\mu (eq_{CH_4})_Z$	·	$\mu (\Delta eq_{CH_4})_N \cdot (1 - \mu (dVFA)_Z)$
5**	$\mu (\Delta q_{IN})_{LN}$	=	$\mu (eq_{CH_4})_Z$	·	$\mu (\Delta eq_{CH_4})_N$
6*	$\mu (\Delta q_{IN})_{LP}$	=	$\mu (eq_{CH_4})_Z$	·	$\mu (\Delta eq_{CH_4})_P \cdot (1 - \mu (dVFA)_Z)$
6**	$\mu (\Delta q_{IN})_{LN}$	=	$\mu (eq_{CH_4})_Z$	·	$\mu (\Delta eq_{CH_4})_P$

660



661 **List of Abbreviations**

- 662 **AD** – Anaerobic Digestion  
663 **AnMBR** – Anaerobic Membrane Bioreactor  
664 **CT** – Conductivity-Transmitter  
665 **EGSB** – Expanded Granular Sludge Blanket  
666 **FIT** – Flow-Indicator-Transmitter  
667 **GC** – Gas Chromatograph  
668 **HN** – High Negative  
669 **HP** – High Positive  
670 **HRT** – Hydraulic Retention Time  
671 **LN** – Low Negative  
672 **LP** – Low Positive  
673 **N** – Negative  
674 **OLR** – Organic Loading Rate  
675 **P** – Positive  
676 **PID** – Proportional-Integral-Derivative  
677 **PIT** – Pressure-Indicator-Transmitter  
678 **PLC** – Programmable Logic Controller  
679 **SRT** – Solid Retention Time  
680 **SR** – Sampling Time  
681 **T** – Temperature Sensor  
682 **UASB** – Up-flow Anaerobic Sludge Blanket  
683 **VFA** – Volatile Fatty Acid  
684 **Z** – Zero  
685

686 **List of Symbols**

- 687  $q_{CH_4}$  – Methane flow rate  
688  $G_{CORRECTED}$  – Corrected biogas flow  
689  $G_{MEASURED}$  – Measured biogas flow  
690  $frho$  – Volumetric correction factor  
691  $\rho_{AIR}$  – Volumetric weight of air  
692  $\rho_{CH_4}$  – Volumetric weight of  $CH_4$   
693  $\rho_{CO_2}$  – Volumetric weight of  $CO_2$   
694  $\rho_{N_2}$  – Volumetric weight of  $N_2$   
695  $eq_{CH_4}(t)$  – Error in methane flow rate at a given time  
696  $q_{CH_4}(t)$  – Methane flow rate at a given time  
697  $q_{CH_4}^*$  – 2-h moving average of  $q_{CH_4}(t)$   
698  $q_{CH_4\_SP}$  – Set-point of methane flow rate  
699  $\Delta eq_{CH_4}(t)$  – Variation in the error of the methane flow rate at a given time  
700  $eq_{CH_4}(t-1)$  – Error in methane flow rate at the previous control action  
701  $\delta$  – Modifying algebraic factor  
702  $dVFA(t)$  – difference between  $VFA_{MAX}$  and the VFA content in the effluent at control time  
703  $VFA(t)$  – Effluent VFA concentration at a given time  
704  $VFA^*$  – 2-h moving average of  $VFA(t)$   
705  $VFA_{MAX}$  – Maximum effluent VFA concentration  
706  $\Sigma eq_{CH_4}(t-1)$  – Accumulated error in methane flow rate at the previous control action  
707  $\Sigma eq_{CH_4}$  – Accumulated error in methane flow rate at a given time  
708  $ST$  – Sampling time  
709  $p$  – Numerical value of a variable  
710  $c$  – Center of the Gaussian-type membership function  
711  $\mu(p)$  – Degree of membership of the input variable  $p$   
712  $\sigma$  – Amplitude of the Gaussian-type membership function  
713  $\Delta q_{CH_4\_SP}$  – Modification in methane flow rate set-point  
714  $q_{IN\_SP}$  – Set-point of influent flow rate  
715  $\Delta q_{IN}$  – Modification of the influent flow rate  
716  $Y_{CH_4}$  – Methane yield